

Electron sound in metals

Yu. A. Avramenko, E. V. Bezuglyi, N. G. Burma, and V. D. Fil'*

B.Verkin Institute for Low Temperature Physics and Engineering, 61103 Kharkov, Ukraine

This paper is devoted to the investigation of electron sound – oscillations of the electron distribution function coupled with elastic deformation and propagating with the Fermi velocity. The amplitude-phase relations characterizing the behavior of the electron sound in Ga single crystals are determined experimentally. A model problem of excitation of electron sound in a compensated metal with equivalent bands is solved for a finite sample with diffusive scattering of electrons at the interfaces. It was found that the displacement amplitude of the receiving interface is two orders of magnitude larger than the elastic amplitude of the wave due to electron pressure. It was established that the changes occurring in the amplitude and phase of the electron sound waves at a superconducting transition do not depend on the path traversed by the wave, i.e. they refer only to the behavior of the transformation coefficient.

I. INTRODUCTION

The existence of different types of waves is characteristic for metals. These are, first and foremost, oscillations of the electron distribution function having velocities close to the Fermi velocity. Initially, it was believed that a necessary condition for their existence is the presence of a magnetic field [1], but it subsequently became clear that some types of waves can also be observed in the absence of a magnetic field. Specifically, the propagation of zero-sound waves is possible for a certain symmetry of the Fermi surface (FS) [2]. If regions between which collisional exchange is impeded for any reason are present on the Fermi surface, then this creates conditions for the existence of a so-called concentration mode [3, 4], which consists of a periodic redistribution of electrons between these regions. Actually, the concentration mode is an electron analog of a first-sound wave. The universal transport mechanism for excitations in a metal with velocities of the order of the Fermi velocity is a quasiwave [5]. A quasiwave process is considered to be a purely ballistic effect, since theoretically it exists in the approximation of noninteracting electrons. The propagation of bunched waves is possible in metals whose Fermi surface contains flat sections [6, 7]. Since the velocity of all these waves is close to the maximum Fermi velocity, Landau damping for them, as a rule, is small and the damping length is of the same order of magnitude as the electron mean free path. Because of the electron and elastic subsystems are quite closely coupled, perturbations of the distribution function are ordinarily accompanied by lattice deformation, i.e. these waves also transfer elastic deformations with the Fermi velocity. This circumstance is essentially the basis for the title of the present article, and it provides the possibility of exciting and detecting them experimentally. These questions have been discussed in detail theoretically and, for the most part, confirmed experimentally.

Our motivation for addressing this well-studied problem is as follows. All theoretical estimates made to date give for the modulus of the coupling coefficient (i.e. the ratio of the amplitude of the elastic displacement in a wave to the amplitude of the exciting signal) $K \sim (s/v_F)^2$ (s is the sound velocity and v_F is the Fermi velocity). However, measurements of the conversion efficiency in different experiments systematically give

values of K which are several tens of times greater than this estimate. This discrepancy has already been noted in a study of fast magnetoplasma waves [8]. A similar picture is also observed for the excitation of zero-sound waves, concentration modes, and quasiwaves. The present work is devoted to an analysis of the reasons for such discrepancies for the example of the excitation of different kinds of waves in ultrapure gallium samples. In the experimental part a careful determination of the conversion efficiency is made, the temperature dependencies of the amplitude-phase characteristics of the elastic disturbances propagating with Fermi velocity are studied, and the effect of a superconducting transition on them is analyzed.

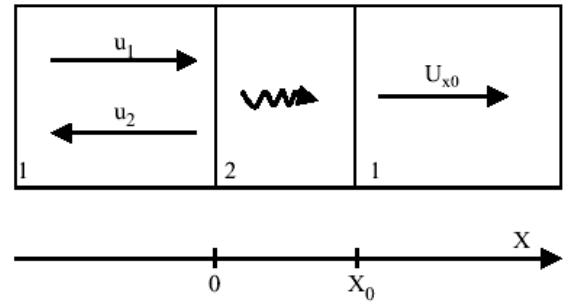


FIG. 1: Simplified scheme of the experiment.

The theoretical part of this work is computational, i.e. it does not contain an analysis of different limiting cases, often difficult to implement in practice, and reduces mainly to a numerical solution of the problem with an experimentally realizable parameter set. It is devoted to two aspects. As far as we know, all theoretical estimates of K have been made for a half-space with a specular boundary. It is naively assumed that the computed amplitude of the elastic field of the electron sound wave is directly detected by the receiving piezoelectric transducer. In the present work the problem is solved for a finite sample with diffusely scattering boundaries. There was an unqualified expectation that taking account of diffuseness will eliminate the discrepancies noted above. In any case the calculations of the efficiency of electromagnetic generation of sound at a diffuse boundary [9] showed that such a possibility does exist. However, it was found that the diffuseness of scat-

tering at the boundary increases K by only several percents. At the same time an analysis of the events on the receiving side revealed that as a result of the considerable difference between s and v_F the receiving interface is an effective concentrator of elastic deformations, increasing by a factor v_F/s compared to the amplitude computed for the interior volume. In other words, the detected elastic displacement is determined not by the magnitude of the elastic deformation in the wave but rather by the much stronger electronic pressure on the interface.

II. SEVERAL EXPERIMENTAL RESULTS

A simplified scheme of the experiment performed in the pulsed regime is presented in Fig. 1. A longitudinal elastic wave with given amplitude U_1 is incident on the delay line-sample exciting interface ($x = 0$) at $t = 0$. Generally, a reflected wave U_2 also exists. The total deformation $U_0 = U_1 + U_2$ acting on the interface excites in the sample a fast electron sound wave and an ordinary sound wave slightly renormalized by the electron-phonon interaction. The arriving electron sound wave engenders a deformation U_{x_0} on the receiving interface ($x = x_0$) at times $x_0/v_F < t < x_0/s$. The delay lines actually used in the experiment to separate fast signals from the probing signal do not have ideal acoustic matching with the sample. However, in the calculations performed in the next section the density of the delay lines and the sample were assumed to be the same and equal to ρ and the sound velocity in them was also assumed to be the same and equal to s , the sound velocity in the sample, in order to avoid analysis of reflections, which in the present case are negligible. In this work the harmonic signals are represented in the form

$$U(t, x) = UK \exp(-\Gamma x) \exp(i\omega t + i\phi), \quad (1)$$

where K is a complex transformation coefficient, Γ is the damping, and ϕ is the phase of the signal. In a propagating wave $\phi = -k'x$ (k' is the real component of the wave number), so that this component of the phase is always negative. The duration of the leading edge of the exciting signal ($\sim 0.2 \mu\text{s}$) is long compared with the period; this makes it possible to neglect in the theoretical analysis the difference of the time derivative from $i\omega$. Figure 2a shows the dependence of the measured amplitude of the fast signals with respect to the excitation amplitude on the thickness of the sample for different frequencies in the most interesting case of waves propagation along the [010] axis. The measurements were performed at temperature 1.7 K, and the impurity relaxation time $\tau \sim 10^{-8}$ s. It is evident that the points fall quite well on a straight line whose slope is frequency-dependent. The extrapolated straight lines converge at $x_0 = 0$ practically to a point, which determines the modulus of the transformation coefficient. Such extrapolation is valid, generally speaking, only for a single excited signal. In a two-signal variant this is possible only if the velocity and damping of the constituent components are close. The frequency dependence of the slopes of the extrapolated straight lines is likewise close to linear

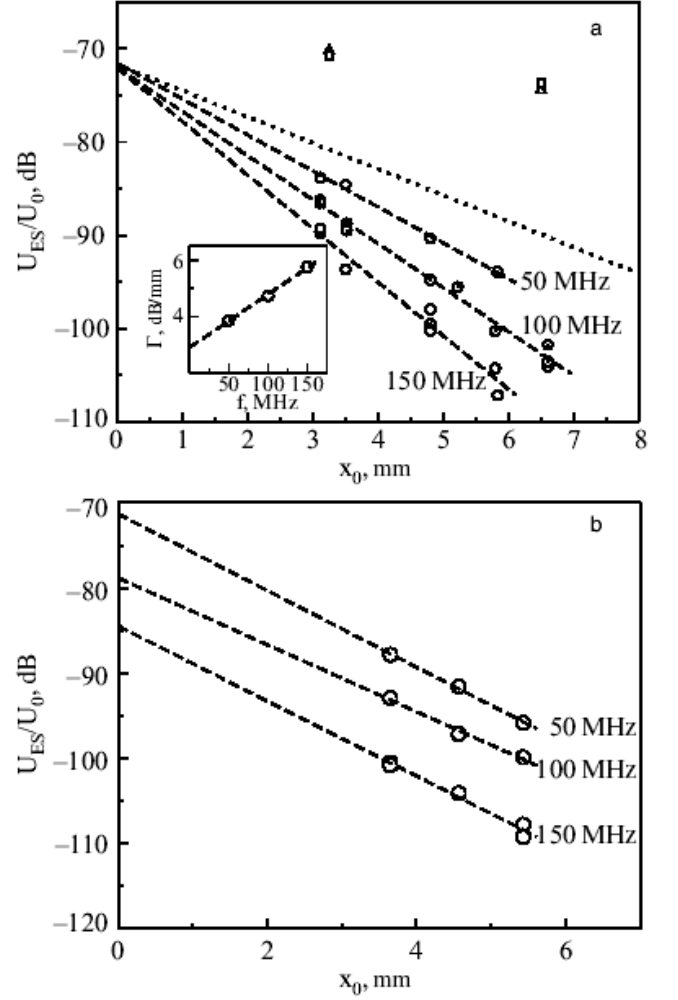


FIG. 2: Measured dependencies of the amplitude of electron sound on the thickness of the sample: $T = 1.7$ K, $\mathbf{q} \parallel [010]$, relaxation damping (points), calculation for $v_1/v_0 = 0.03$, $F = 1$ (\square), $v_1/v_0 = 0.03$, $F = 0.01$ (\triangle) (a). Inset: dependence of the damping on the frequency. Measured dependencies of the amplitude of electron sound on the thickness of the sample: $T = 1.7$ K, $\mathbf{q} \parallel [100]$ (b).

(inset in Fig. 2a), which is, most likely, an indication that Landau damping is weak. The intersection of this line with the ordinate determines the frequency-independent relaxation damping, agreeing well with the known relaxation time with $v_F \approx 7 \times 10^7$ cm/s. The contribution of the relaxation exponent is presented in Fig. 2a (dotted line).

Similar results for the [100] axis are presented in Fig. 2b. Here, once again, the thickness dependences can be represented by straight lines. However, in contrast to the [010] axis the slopes of these straight lines are practically frequency-independent and are close in magnitude to the slope determined by the relaxation damping. At the same time the conversion coefficient determined by the coordinates of the intersection of the straight lines with the ordinate is frequency-dependent, though the value is close to that measured on the [010] axis. Apparently, here the situation is close to the two-

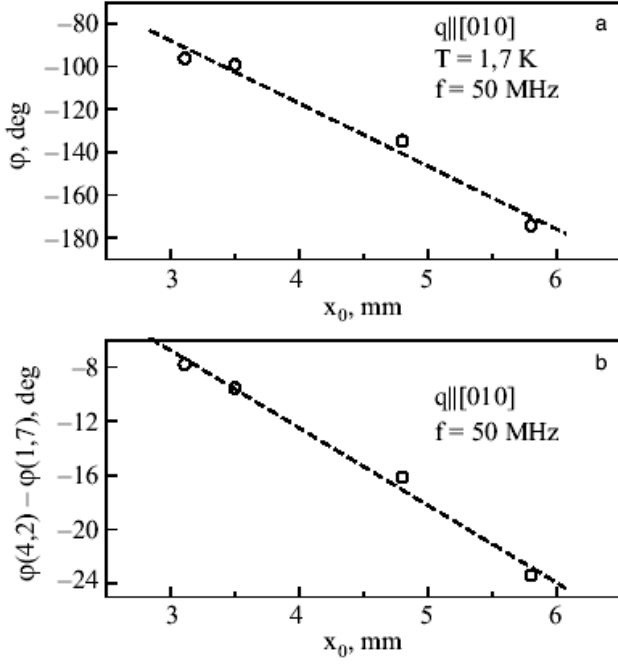


FIG. 3: Measured sample thickness dependences of the phase: total change of the phase (a); the phase increment accompanying a temperature change from 1.7 to 4.2 K (b).

signal case with a frequency-dependent phase difference between the constituent components.

We shall now discuss the phase characteristics of the signals. It is hardly possible to determine the reference point experimentally with adequate accuracy. For this reason only relative measurements are meaningful. Figure 3a shows the thickness dependence of the phase which the electron sound wave acquires as it propagates along the [010] axis. A straight line also fits it well, its slope giving a wave velocity close to 7×10^7 cm/s at $T = 1.7$ K. The phase of the signals decreases with increasing temperature; this indicates either a change of the velocity of the electron sound wave or a strong dependence of the phase of the transformation coefficient on the relaxation time. It has been shown in a previous work [4] that a substantial decrease of the velocity is possible only in a two-band model of the spectrum with strongly impeded interband scattering (to a level of several percent of the intraband scattering), which, at first glance, appeared to be quite unusual. One of our tasks in the present work was to separate two possible contributions to the change of the total phase of the electron sound wave. Figure 3b shows the thickness dependence of the temperature increments to the phase. Evidently, the straight line fit has a nonzero slope, indicating that the wave velocity decreases by 20%. At the same time, the nonzero coordinate of intersection of the straight line and the ordinate likewise attests to a simultaneous small increment to the phase of the transformation coefficient.

More detailed information can be obtained from the temperature dependences of the phase of the signal in samples of

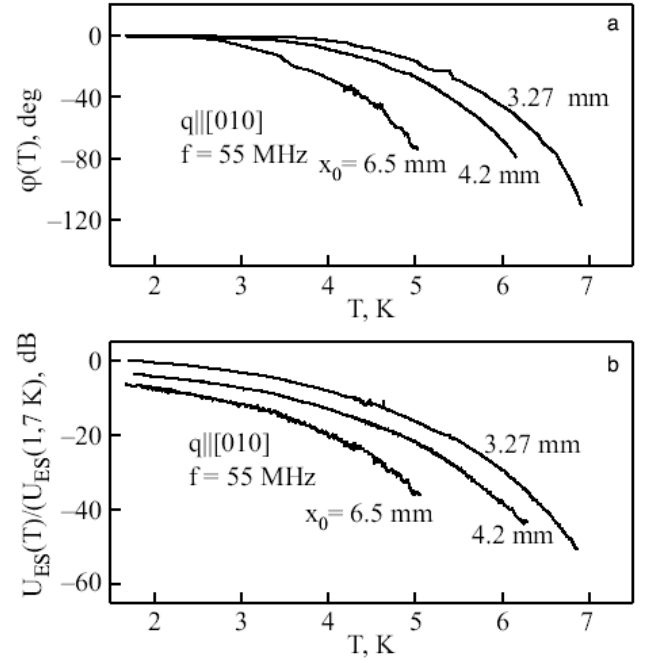


FIG. 4: Temperature dependences of the amplitude-phase characteristics of electron sound: phase change measured from 1.7 K (a); amplitude change (the curves are shifted by 4 dB) (b).

different length. Figure 4a shows the phase changes measured from the level at $T = 1.7$ K ([010] axis). The change of the electron sound velocity can be found by representing the signals in the form (1). A decrease of τ to 10^{-9} s ($T \sim 5$ K) results in a gigantic (40%) decrease in the velocity (Fig. 5a). The phase of the transformation coefficient increases somewhat as τ decreases (Fig. 5b). The amplitude dependences are presented in Fig. 4b. Analysis shows that the change in modulus of the transformation coefficient in the limit of the measurement error is negligible.

The phenomena described above are absent for waves propagating in the [100] direction – the phases remain practically unchanged right up to vanishing of the signals.

In concluding this section we wish to emphasize the essential experimental facts: 1. the modulus of the transformation coefficient at $T=1.7$ K ($\tau \sim 10^{-8}$ s) lies in the range $-70 \dots -80$ dB; 2. the velocity of electron sound waves propagating in the [010] direction depends strongly on the relaxation rate, dropping by approximately 40% at $\tau \sim 10^{-9}$ s; and 3. the phase of the transformation coefficient increases somewhat (~ 20 deg) with increasing scattering.

III. THEORETICAL ANALYSIS

The one-dimensional kinetic equation, describing the process, for the nonequilibrium correction $\psi(x)$ to the distribution function $n = n_F(E) + (\partial n_F / \partial E) \psi$ ($n_F(E)$ is the Fermi

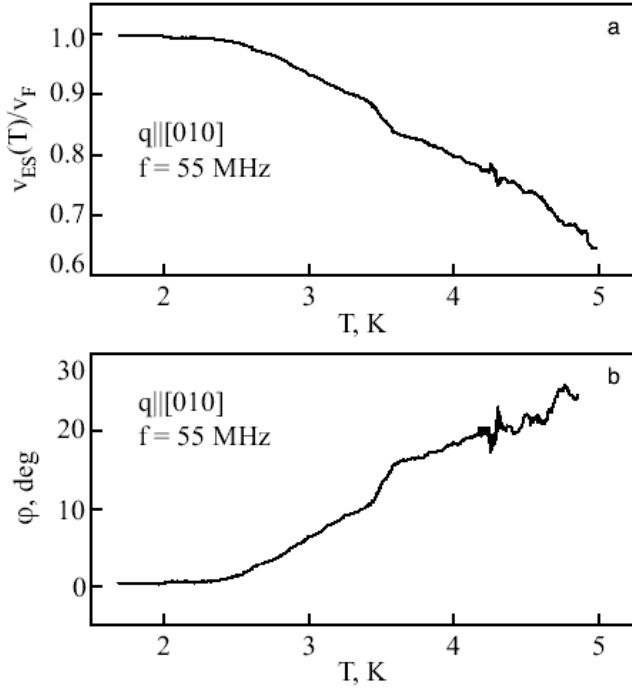


FIG. 5: Temperature dependence of the electron sound velocity (a) and of the phase of the transformation coefficient (b).

function of the total quasiparticle energy E) has the form

$$i\omega(1 + \hat{f})^{-1}\psi + v \frac{\partial}{\partial x}(\psi - e\phi) + i\omega\Lambda \frac{\partial U}{\partial x} = I(\psi). \quad (2)$$

Here $v = v_{Fx}$ and $\Lambda = \Lambda_{xx}$ are the longitudinal components of the electron velocity and the deformation potential, ϕ is the electric potential, \hat{f} is the Fermi-liquid interaction (FLI) operator, U is the elastic deformation, and $I(\psi)$ is the collision integral which takes account of the law of conservation of the number of particles during scattering [10]

$$I_\alpha(\psi) = \sum_\beta w_{\alpha\beta} \left(\langle \psi \rangle_\beta - N_{F\beta} \psi_\alpha \right). \quad (3)$$

Here and below Greek indices enumerate the electronic groups, $w_{\alpha\beta} = w_{\beta\alpha}$ is the scattering (assumed to be isotropic for simplicity) probability matrix, the brackets signify integration over the FS in the α th zone

$$\langle \mu \rangle_\alpha \equiv \frac{2}{(2\pi\hbar)^3} \int_{\mathbf{p} \in \alpha} \frac{dS_{\mathbf{p}}}{v_F} \mu(\mathbf{p}),$$

and $N_{F\alpha} = \langle 1 \rangle$ is the density of states in the α th zone. In the model examined below, which takes account of only the isotropic part of Landau correlation function, the action of the operator \hat{f} on an arbitrary function $\mu(\mathbf{p})$ of the quasimomentum \mathbf{p} in the α th zone is determined by the relation

$$(\hat{f}\mu)_\alpha = (\hat{f}\langle \mu \rangle)_\alpha \equiv \sum_\beta f_{\alpha\beta} \langle \mu \rangle_\beta,$$

where $f_{\alpha\beta} = f_{\beta\alpha}$ is the matrix of the coefficients of the FLI.

To find a relation between the electric and elastic fields the kinetic equation (2) must be supplemented by the electroneutrality condition

$$\sum_\alpha \langle (1 + \hat{f})^{-1} \psi \rangle_\alpha = 0,$$

which in the geometry under consideration reduces to the condition for the absence of a longitudinal current

$$\sum_\alpha \langle v\psi \rangle_\alpha = 0, \quad (4)$$

as well as an equation from the theory of elasticity that takes account of the contribution of the force f_e exerted by the electrons on the vibrating lattice [11, 12]:

$$\begin{aligned} \omega^2 U &= -s^2 \frac{\partial^2 U}{\partial x^2} + f_e, \\ f_e &= \rho^{-1} \frac{\partial}{\partial x} \sum_\alpha \langle \Lambda(1 + \hat{f})^{-1} \psi \rangle_\alpha \equiv \rho^{-1} \frac{\partial W}{\partial x}. \end{aligned} \quad (5)$$

In what follows, as in Ref. 3 and 4, we shall examine a simplest model of a compensated metal with equivalent e and h spherical Fermi surfaces ($v_{Fe} = v_{Fh}$, $N_e = N_h$, and $\Lambda_e = -\Lambda_h$) with the difference between the intra- and interband FLI coefficients and the corresponding scattering rates being preserved. It is obvious that for such a symmetry of the problem $\psi_e = -\psi_h$ and $\phi = 0$. As a result, it is sufficient to study the solution of the kinetic equation for a single sheet of the FS, doubling f_e in the elasticity equation (5). In addition, since the value of the nonrenormalized deformation potential averaged over both bands is zero, we have $\Lambda_{xx} = mv_x^2$. We introduce the following notations:

$$\begin{aligned} F_{ee} = F_{hh} = F_0, \quad F_{eh} = F_1, \quad F = F_0 - F_1, \quad F_{\alpha\beta} = N_F f_{\alpha\beta}, \\ v_{ee} = v_{hh} = v_0, \quad v_{eh} = v_1, \quad v_{\alpha\beta} = N_F w_{\alpha\beta}. \end{aligned} \quad (6)$$

Taking account of the simplifications following from the model the kinetic equation becomes

$$\begin{aligned} i\omega(1 + \hat{f})^{-1}\psi + v \frac{d\psi}{dx} &= -i\omega\Lambda \frac{dU}{dx} - v^+ \psi + v^- \frac{\langle \psi \rangle}{N_F} \\ v^\pm &= v_0 \pm v_1. \end{aligned} \quad (7a)$$

Applying the operator $(1 + \hat{f})$ to the left hand side, we arrive at the equation

$$\begin{aligned} i\tilde{\omega}\psi + v \frac{d\psi}{dx} &= -i\omega\Lambda \frac{dU}{dx} - v^+ \psi + v^- \langle \psi \rangle \frac{\omega^-}{N_F} \equiv A(x), \\ i\tilde{\omega} &= i\omega + v^+, \quad \omega^- = v^- + \frac{i\omega F}{1 + F} \equiv v^- + i\omega F_2. \end{aligned} \quad (7b)$$

The solution of Eq. (7b) in the coordinates of Fig. 1 has the form

$$\psi_{v>0} = C e^{-Lx} + e^{-Lx} \int_0^x \frac{A(x')}{v} e^{Lx'} dx', \quad L = \frac{i\tilde{\omega}}{v}, \quad (8a)$$

$$\psi_{v<0} = C_1 e^{-L(x-x_0)} + e^{-Lx} \int_{x_0}^x \frac{A(x')}{v} e^{Lx'} dx'. \quad (8b)$$

The solution (8a) and (8b) is suitable for any kind of the scattering boundary. For diffusive scattering, C_1 and C are “true” constants, while for specular scattering they are functions of v . We shall assume that the exciting boundary ($x = 0$) is diffusive (i.e. C is a constant), and for now we shall not specify the type of the reflection at the receiving interface.

The average value $\langle \psi \rangle$ can be represented in the form [13]

$$\langle \psi \rangle = C \langle e^{-Lx} \rangle_{>} - \langle C_1 e^{-L(x-x_0)} \rangle_{<} + \left\langle \int_0^{x_0} \frac{A(x')}{v} e^{-L|x-x'|} dx' \right\rangle. \quad (9)$$

The subscripts indicate the part of the Fermi sphere (the sign of the longitudinal component of the Fermi velocity) over which the averaging is performed; the absence of a subscript means that the averaging is performed over the entire zone. We shall find W by averaging the expression (7a) with the weight Λ and using (7b) to determine $\langle \Lambda v d\psi/dx \rangle$:

$$\frac{W}{2} = \langle \Lambda \psi \rangle - F_2 \langle \Lambda \rangle \frac{\langle \psi \rangle}{N_F} = C \langle \Lambda e^{-Lx} \rangle_{>} + \langle C_1 \Lambda e^{-L(x-x_0)} \rangle_{<} + \left\langle \Lambda \int_0^{x_0} \frac{A(x')}{v} e^{-L|x-x'|} dx' \right\rangle_{>} - F_2 \langle \Lambda \rangle \frac{\langle \psi \rangle}{N_F}. \quad (10)$$

We shall solve the problem in the Fourier representation by the Wiener-Hopf method [14], assuming all physical fields outside the sample to be zero. To use the properties of a convolution, we extend the definition the integrals on the right-hand sides of Eqs. (9) and (10) over the entire x axis, adding and subtracting the corresponding functions

$$\begin{aligned} \langle \psi \rangle_k &\equiv \int_0^{x_0} \langle \psi \rangle e^{-ikx} dx = C \left\langle \frac{1 - e^{-(L-ik)x_0}}{L + ik} \right\rangle_{>} \\ &- \left\langle \frac{C_1 (e^{-ikx_0} - e^{-Lx_0})}{L + ik} \right\rangle_{<} + \left\langle \frac{A_k}{v} \frac{2L}{L^2 + k^2} \right\rangle_{>} \\ &- \left\langle \frac{\alpha_1}{v(L-ik)} \right\rangle_{>} - \left\langle \frac{\alpha_2 e^{-(L+ik)x_0}}{v(L+ik)} \right\rangle_{>}, \\ \alpha_1 &= \int_0^{x_0} A(x') e^{-Lx'} dx', \quad \alpha_2 = \int_0^{x_0} A(x') e^{Lx'} dx', \quad (11) \end{aligned}$$

where A_k is the Fourier component of $A(x)$.

The last two terms in Eq. (11) are analytic for $k'' = \text{Im} k > -v^+/v$ and $k'' < v^+/v$, respectively:

$$\begin{aligned} \frac{W_k}{2} &= C \left\langle \frac{\Lambda (1 - e^{-(L+ik)x_0})}{L + ik} \right\rangle_{>} - \left\langle \frac{C_1 \Lambda (e^{-ikx_0} - e^{-Lx_0})}{L + ik} \right\rangle_{<} \\ &+ \left\langle \frac{A_k}{v} \frac{2\Lambda L}{L^2 + k^2} \right\rangle_{>} - \left\langle \frac{\Lambda \alpha_1}{v(L-ik)} \right\rangle_{>} \\ &- \left\langle \frac{\Lambda \alpha_2 e^{-(L+ik)x_0}}{v(L+ik)} \right\rangle_{>} - F_2 \langle \Lambda \rangle \frac{\langle \psi \rangle_k}{N_F}. \quad (12) \end{aligned}$$

The Fourier transform of the elasticity equation has the form

$$i(q^2 - k^2)U_k = (k - q)U_{x_0} e^{-ikx_0} - (k + q)U_0 + 2qU_1 - \frac{kW_k}{\rho s^2}, \quad (13)$$

where $q = \omega/s$ is the wavenumber of the sound. The relation (13) was obtained using the boundary conditions for the displacement $U_0 = U_1 + U_2$ and for the elastic stress

$$-iqU_1 + iqU_2 = \frac{dU_0}{dx} - \frac{W(0)}{\rho s^2} \quad (x = 0), \quad (14a)$$

$$-iqU_{x_0} = \frac{dU_{x_0}}{dx} - \frac{W(x_0)}{\rho s^2} \quad (x = x_0). \quad (14b)$$

We call attention to the fact that the derivatives on the left and right hand sides in the boundary conditions are calculated on different sides of the interface, and they are by no means equal. Using the identities

$$\begin{aligned} \left\langle \frac{\Lambda}{L + ik} \right\rangle &= \varepsilon \left\langle \frac{L - ik}{L^2} - \frac{1}{L + ik} \right\rangle, \quad \varepsilon = \frac{E_F k_0^2}{k^2}, \\ \left\langle \frac{\Lambda L}{L^2 + k^2} \right\rangle &= \varepsilon \left\langle \frac{1}{L} - \frac{L}{L^2 + k^2} \right\rangle, \quad k_0 = \frac{i\tilde{\omega}}{v_F}, \quad E_F = mv_F^2, \end{aligned}$$

we obtain

$$\begin{aligned} \frac{W_k}{2} &= -\varepsilon \left[\langle \psi \rangle_k T(k) + I_0(k) + I_1(k) e^{-ikx_0} + 2 \langle \Lambda \rangle \frac{\omega}{\tilde{\omega}} \right. \\ &\times \left. \left(U_{x_0} e^{-ikx_0} - U_0 + ikU_k \right) \right], \quad T(k) = 1 - \frac{\omega^-}{\tilde{\omega}} + \frac{F_2}{3} \frac{k^2}{k_0^2}, \\ I_0(k) &= C \left\langle \frac{L - ik}{L^2} \right\rangle_{>} + \left\langle \frac{C_1 (L - ik)}{L^2} \right\rangle_{<} - \left\langle \frac{\alpha_1 (L + ik)}{vL^2} \right\rangle_{>}, \\ I_1(k) &= -C \left\langle \frac{e^{-Lx_0} (L - ik)}{L^2} \right\rangle_{>} + \left\langle \frac{C_1 (L - ik)}{L^2} \right\rangle_{<} \\ &- \left\langle \frac{\alpha_2 e^{-Lx_0} (L - ik)}{vL^2} \right\rangle_{>}, \quad (15) \end{aligned}$$

Substituting the expressions (15) into the elasticity equation and transferring to the left-hand side the terms with U_k and $\langle \psi \rangle_k$ and all terms containing e^{ikx_0} we obtain

$$\begin{aligned} k\Delta(k)U_k - \frac{i\sigma k_0^2}{n} T(k) \langle \psi \rangle_k + \left[-ik(k - q)U_{x_0} + \frac{ik_0^2}{n} I_1(k) \right. \\ \left. + \sigma k_F k_0 U_{x_0} \right] e^{-ikx_0} = -ik(k + q)U_0 + 2ikqU_1 \\ - \frac{i\sigma}{n} k_0^2 I(k) + \sigma k_F k_0 U_0, \quad \Delta(k) = k^2 - q^2 + i\sigma k_F k_0 \quad (16) \end{aligned}$$

where $k_F = \omega/v_F$ should not be confused with the Fermi momentum, $\sigma = E_F/Ms^2$, M is the ion mass, and n is the carrier density in the zone. The parameter σ in the free-electron model is close to 1 but in a real case, because of the electron-phonon renormalization of the Fermi surface, as a rule, it is less than 1. In what follows $\sigma = 0.25$ is used in numerical estimates.

The function on the right-hand side of Eq. (16) is analytic on the entire complex plane and by Liouville's theorem can be represented as a quadratic polynomial:

$$\begin{aligned} P_2(k) &= \alpha k^2 + \beta k + \gamma, \\ \alpha &= -iU_0, \quad \gamma = \sigma k_F k_0 U_0 - \frac{i\sigma k_0^2}{n} I_0(0). \end{aligned}$$

The left-hand side of Eq. (16) contains terms which increase exponentially as $k'' \rightarrow -\infty$. Evidently, in order for the relations (16) to hold U_k and $\langle \psi \rangle_k$ finite, they must contain components that exactly compensate this growth. Then the relation (16) can be split into two independent equations and each equation can be solved separately. Such splitting makes it possible to circumvent the inconveniences due to the absence of singular points in the Fourier transforms taken on a finite interval and to make use of contour integration to obtain the inverse transform. Likewise, the physical meaning of the terms containing the factor $\exp(-ikx_0)$ is obvious: when the inverse transformation is computed the contour integrals with the factor $e^{-ik(x_0-x)}$ ($x < x_0$) must be closed in the bottom half-plane in k space; this corresponds to waves propagating in the negative x direction.

Eliminating $\langle \psi \rangle_k$ for forward waves from Eqs. (11) and (16) we obtain

$$\begin{aligned} Z(k)[kB_z(k)U_k - V_0(k)] &= 3\sigma k_0^2 T(k)d[k_F k_0 q^2 U_0 \\ &+ k\Delta(k)C + ikk_F k_0 \beta + \frac{k_F k_0^3}{n} I_0(0)] + \frac{i\sigma k_0^2}{n} T(k)B_z(k)J_0(k), \\ V_0(k) &= P_2(k) \frac{\omega^-}{i\omega} k^2 - 3\sigma k_F k_0^3 T(k)U_0 - 3\sigma k k_0^2 T(k) \frac{C}{E_F}, \\ B_z(k) &= \frac{\omega^-}{i\omega} k^2 \Delta(k) - 3i\sigma k_F k_0^3 T(k), \\ J_0(k) &= C \left\langle \frac{1}{L-ik} \right\rangle_+ + \left\langle \frac{C_1 e^{-Lx_0}}{L+ik} \right\rangle_- - \left\langle \frac{\alpha L}{v(L-ik)} \right\rangle_+, \\ Z(k) &= d\Delta(k) + B_z(k) \left\langle \frac{1}{L^2 + k^2} \right\rangle_+, \quad d = 1 - \frac{\omega^-}{i\omega}. \end{aligned} \quad (17)$$

The characteristic equation $Z(k) = 0$ determines the wave-numbers of the propagating waves. In general, there are two pairs of roots: $r_1 \approx \pm k_0$ and $r_2 \approx \pm q$ – sound slightly renormalized by the electron-phonon interaction. In addition, there

are two branch points $k = \pm ik_0$ with which the quasiwave process is associated.

Let the roots r_1 and r_2 ($\text{Re } r_{1,2} < 0$, $\text{Im } r_{1,2} > 0$) lie in the upper half-plane. According to the Wiener-Hopf method, the function $Z(k)$ must be factorized, i.e. represented as a product of two functions which are analytic, respectively, in the upper and lower half-planes and have a common strip of analyticity. The function $Z(k)$ has no singularities near the real axis, including $k = 0$. As $k \rightarrow \infty$, $Z(k)$ behaves as k^2 . We introduce the function

$$\tilde{Z}(k) = \frac{Z(k)}{(k+r_1)(k+r_2)},$$

which can be factorized according to a general rule [14], $Z(k) = \tau^+(k)\tau^-(k)$, where

$$\tau^+(k) = \exp \left(\frac{1}{2\pi i} \int_{-\infty+i\delta}^{+\infty+i\delta} \frac{\ln \tilde{Z}(\xi)}{\xi - k} d\xi \right). \quad (18)$$

Since the poles of $Z(k)$ in the function $\tilde{Z}(k)$ for $k'' < 0$ have already been eliminated, the calculation of the integral (18) by closing the contour in the lower half-plane reduces to the contribution of only the cut C' , extending from the point ik_0 to infinity. To choose the cut C' it is necessary to make sure that the integrand does not cross the cut itself, accompanied by a jump of the imaginary part of the logarithm. Specifically, the commonly used variant where the cut is drawn along a ray emanating from the coordinate origin and passing through the branch point does not work in the present case. Any cut made near the imaginary axis will work.

For waves propagating in the forward direction the amplitude behaves as $e^{-\Gamma x}$ ($\Gamma > 0$), so that U_k is analytic for all $k'' < \Gamma$. Dividing (17) by $(k+r_1)(k+r_2)\tau^+(k)$, we obtain the functional equation

$$\tau^-(k)[kB_z(k)U_k - V_0(k)] = - \frac{3\sigma k_0^2 T(k)dk_F k_0 q^2 U_0 + k\Delta(k)C + ikk_F k_0 \beta + \frac{k_F k_0^3}{n} I_0(0)}{(k+r_1)(k+r_2)\tau^+(k)} + \frac{i\sigma}{n} \frac{k_0^2 T(k)B_z(k)J(k)}{(k+r_1)(k+r_2)\tau^+(k)}. \quad (19)$$

The left- and right-hand sides of Eq. (19) are analytic, respectively, in the lower and upper half-planes, they possess a common strip of analyticity near the real axis, and they can be represented as cubic polynomials

$$P_3(k) = T(k)(A_1 k + A_0).$$

Setting $k = 0$ and using $I_0(0) = J_0(0)$ we obtain

$$A_0 = - \frac{2\sigma k_F k_0^3 d}{r_1 r_2 \tau^+(0)} q^2 U_0. \quad (20)$$

We find the coefficient A_1 as well as the unknown constants

C , β , and $I_0(0)$ by setting k equal to the roots b_i of the quartic polynomial $B_z(k)$.

We call attention to a paradoxical, at first glance, circumstance. Even though x_0 appears explicitly in $I_0(0)$, this constant does not depend on x_0 , just as it does not depend on C_1 or on the character of the reflections at the receiving interface. The situation is that these quantities also appear in α_1 , since as one can see from Eq. (11), α_1 is the $(-iL)$ th Fourier component of the perturbing field $A(x)$, which is determined by the contribution of the forward and backward waves. The independence of $I_0(0)$ from x_0 and C_1 shows that the contribution

of the backward wave to $I_0(0)$ is completely annihilated. Of course, this does not mean that the field of the forward wave is absolutely insensitive to the distance up to the receiving interface and the character of the reflections from it. In reality, the amplitudes of the propagating waves are determined in terms of the field on the emitting boundary U_0 and, naturally, the backward wave contributes to it. But, as will become clear below, this correction is $\sim (s/v_F)^2$ for a diffuse boundary at $x = x_0$ and, apparently, $\sim s/v_F$ for a specular boundary.

Thus the elastic field of the forward wave at any point of the sample is practically independent of the thickness of the latter and can be calculated using the relations obtained for a half-space. The Fourier transform of the elastic component of the field of the forward wave has the form

$$U_{k1} = \frac{T(k)(A_1 k + A_0)(k + r_1)(k + r_2)\tau^+(k)}{kB_z(k)Z(k)} + \frac{V_0(k)}{kB_z(k)}. \quad (21a)$$

In Eq. (21a) $\tau^-(k)$ is replaced by

$$\frac{Z(k)}{(k + r_1)(k + r_2)\tau^+(k)}.$$

It is easy to show that $k = 0$ and $k = b_i$ are not poles of U_{k1} and the physical fields are determined only by the roots and branch point of $Z(k)$. The amplitude of the sound wave is practically equal to U_0 , while the electron sound wave of interest to us is the total contribution of the mode with $k = r_1$ (if this root exists) and a quasiwave.

The Fourier transform of the elastic component for the half-space with a specular interface boundary is calculated in Refs. 3 and 4. In our notation it has the form

$$U_{k1} = -\frac{6\sigma k_F k_0^3 T(k) dq^2 U_0}{kB_z(k)Z(k)}. \quad (21b)$$

The terms eliminating the singularities at $k = 0$ and $k = b_i$ have been dropped in Eq. (21b).

The term with A_0 makes the main contribution to the polynomial $P_3(k)$ at $k \sim k_0$, so that both solutions (21a) and (21b) are practically identical even in the literal form. Figures 6 shows for a concrete parameter set the ratio of the moduli of the signals and their phase difference, which are calculated using the relations (21a) and (21b). It is evident that even diffuseness results in a very small increase of the transformation efficiency. But the magnitude of the total signal itself, calculated, for example, for $x_0 = 3$ mm, at $T = 1.7$ K and $v_F/s = 200$ is -110 dB, which is much less than the experimental values (see Fig. 2).

We shall now discuss the events which occur on the receiving interface. If the reflections on it are diffuse, the constant C_1 is independent of v and can be removed from the averaging operation. The functional equation determining the Fourier transform of the backward waves is identical to, with the exception of the common factor $\exp(-ikx_0)$, some relabeling, and mutual substitutions of the regions of analyticity, the expression (19) with $-U_{x_0}$ replacing U_{x_0} . This means that the as yet unknown elastic displacement U_{x_0} arising at the interface

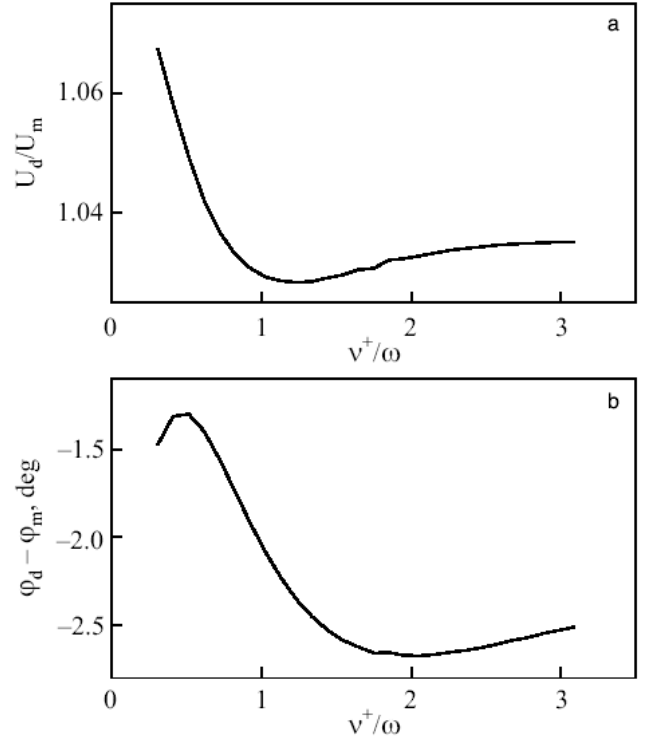


FIG. 6: Comparison of the results for diffuse (d) and specular (m) boundaries: $v_1/v_0 = 0.03$, $F = 0.6$; the quantity $k_F x_0 = 1.2$, corresponding to $x_0 \sim 0.33$ cm, was used in the calculation; amplitude ratio (a) and phase difference (b).

engenders backward waves with the same efficiency as the initial perturbations at $x = 0$. Specifically, the main contribution to the waves moving away from the boundary will be acoustic with amplitude practically the same as U_{x_0} . The relation between U_0 and U_{x_0} is determined by the condition of continuity of the elastic stresses on both sides of the interface (14b). The derivative dU_{x_0}/dx can be replaced by $-ir_2 U_{x_0} \approx iq U_{x_0}$, and only the arriving electron sound wave need be taken into account in the electron-elastic potential $W(x_0)$. According to Eq. (13) the Fourier transform W_k has the form

$$-\frac{W_k}{\rho s^2} = \frac{(k^2 - q^2)U_{k1}}{ik}. \quad (22)$$

All terms which are unrelated to the singular points of $Z(k)$ have been dropped in Eq. (22). Using the representation of U_{k1} found above, the inverse Fourier transform makes it possible to find $W(x_0)$. Since the characteristic $k \approx k_0 \ll q$ in the electron sound wave incident on the boundary, we obtain for the amplitude of the elastic field

$$U_{x_0} \sim \frac{v_F}{2s} U_f \approx \frac{s}{2v_F} U_0,$$

where U_f is the displacement amplitude in the incident wave.

We arrive at the following conclusion, which is the essential result of the present work – the experimentally recorded

displacements engendered by the electron sound wave are determined by, first and foremost, the electronic pressure on the boundary and are substantially greater than the elastic component of the wave itself. Although this result was obtained for a specific model of a compensated metal with equivalent bands, its validity evidently is not limited by the properties of this particular model.

In the case of specular reflection, aside from the incident electronic waves, reflected waves with amplitude comparable to the first waves and also contributing to $W(x_0)$ also appear. This complicates the solution of the problem. However, if the structure of the elastic field arising in the metal is ignored and only the magnitude of the signal on the receiving interface is considered, then we can use the reciprocity principle [15]. According to this principle, if the transmitting medium is not gyrotropic and no linear effects occur in it, then the recorded amplitude is independent of which piezoelectric transducer is the source of the perturbation and which is the receiver. Since, as the preceding discussion has made clear, the scale of the events at a diffuse boundary is independent of the specularity of the generating interface, exactly the same result must obtain in the opposite case.

We shall now briefly discuss the qualitative results following from the calculations performed above and from their comparison with experiment. Figures 7 and 8 demonstrate the typical computed dependences of the amplitude and phase of the elastic displacement, recorded on the receiving interface for the cases of weak and intense interband scattering. The results are presented in the interval of total relaxation rates which is close to the experimental interval. It was assumed in the calculations that the ratio v^-/v^+ is independent of the temperature. The contribution of the pole (if it exists), the contribution of the branch point, and the total signal were presented separately. The contribution of the pole is usually identified with zero sound in the limit of weak scattering and with the concentration mode in the opposite case [3, 4]. In what follows, for brevity, this contribution will be called the wave component. The contribution of the branch point will be called the quasiwave part, which conforms to the accepted terminology [5]. The interband scattering parameter (Figs. 6 and 7) was chosen, as done previously in Ref. 4, so that it would describe the actually observed decrease of the electron sound velocity $q||[010]$. The essential conclusions following from the calculations performed reduce to the following.

1. For a given interband scattering rate the amplitude of the total signal is practically independent of the FLI parameter (see also Fig. 2). At the same time a change of F results in a redistribution of the intensities between the wave component and the quasiwave. For weak interband exchange in the region of existence of the concentration mode (high temperatures) the latter always dominates with the exception of v^+ adjoining the boundary of its existence. The wave component also predominates for low temperatures and $F \geq 0.6$. The quasiwave predominates for intense interband exchange and small F , but for $F \sim 1$ and small v^+ the zero-sound solution makes the main contribution. There exists a theorem

asserting that in the degenerate case of the type studied in the present work and in the absence of scattering zero sound exists for arbitrarily weak FLI [2]. The result presented in Fig. 7b agrees with this assertion, but the amplitude of the wave component is small and is completely masked by the quasiwave.

2. In spite of the existence of jumps in the behavior of individual signal components that are associated with the vanishing of the pole due to the wave component, the total displacement demonstrates absolutely monotonic variation of the amplitude-phase characteristics and their derivatives. The existence of such compensation within the framework of similar model was first noted in Ref. 3. Apparently, this feature is not associated with the particular choice of the form of the FS. We performed calculations for an FS with different configuration – cylinders with spherical “caps” at the ends, and we obtained exactly the same result. In our opinion such ideal “interchangeability” attests to the fact that both components actually describe the same process. Their separation into wave and quasiwave components does have any profound physical meaning and is no more than a mathematical device.

3. The phase of the transformation coefficient. From the theoretical standpoint it should be defined as the phase of the total signal at $x_0 = 0$. However, experimentally, it was determined according to the scheme $\arg K = 2 \arg U(x_0) - \arg U(2x_0)$. For a linear phase characteristic these definitions are equivalent, but because of the fundamentally existing deviations from linearity the answers differ somewhat. Figure 9 shows the phase of K calculated using the experimental scheme. In the model under discussion a sign change of the phase with increasing scattering that agrees with the observed change (Fig. 5b) cannot be obtained for any combination of parameters. At the same time we note that the phases of both components forming the total signal increase with increasing scattering – a simply rapid drop of the amplitude of the quasiwave masks the phase increase in the resulting signal. One possible reason for the observed discrepancy could be that initially the magnitude of the quasiwave component is understated because of the diffraction losses for it and for the wave component.

There arise completely natural questions of whether the FLI has an effect at all on the process of excitation and propagation of electron sound and whether it is possible to estimate its intensity on the basis of experiments similar those which have been performed. The answer to the first question is yes – the FLI is the source of the force that supplements the forces existing in the gas model. As a result, the stiffness of the system increases, manifesting in the propagation velocity of the waves. Figure 10 shows the computed electron sound velocities which were obtained by differentiating the phase of the total signal with respect to x_0 . Independently of the intensity of the interband exchange, the velocity of the signals increases with increasing F . These changes are quite large and can be easily recorded, but the absence of a model-independent point of reference actually precludes the possibility of estimating F from these experiments. The possibility of separating the wave and quasi-wave components according to the sign of

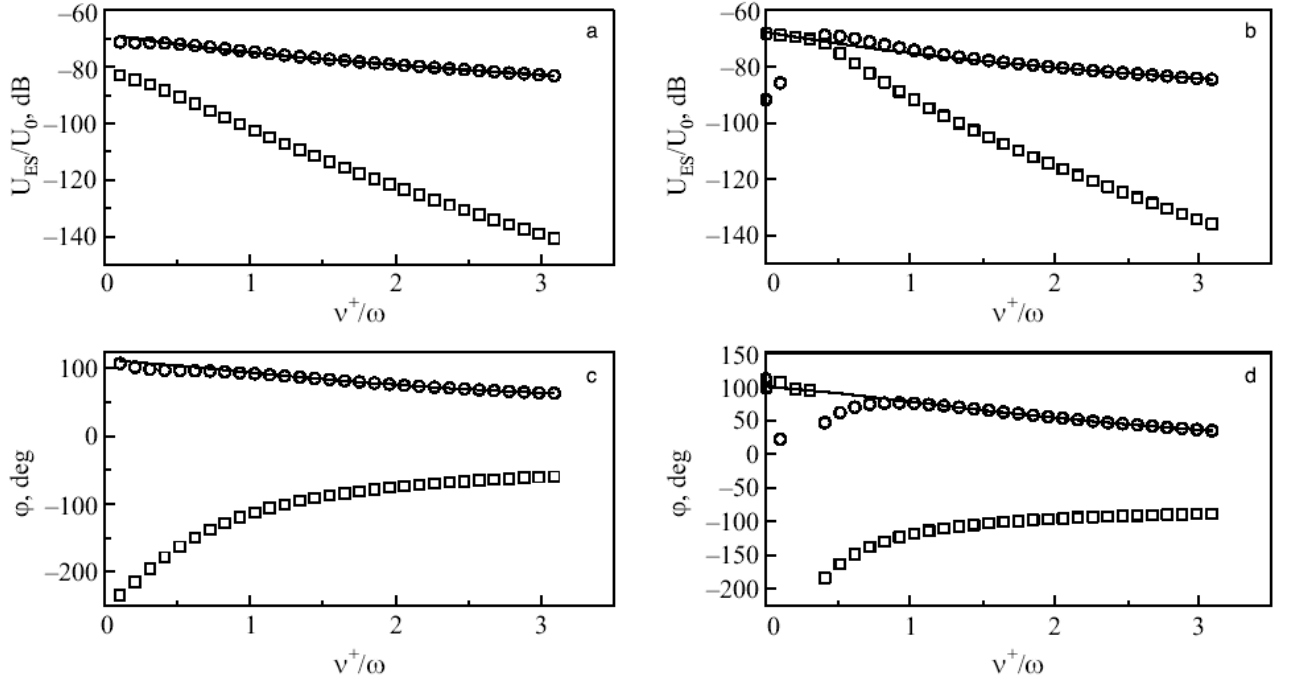


FIG. 7: Computed dependences of the amplitude and phase of electron sound with weak interband exchange $v_1/v_0 = 0.03$ versus the scattering parameter $k_F x_0 = 1.2$: wave component (\circ), quasiwave component (\square), total signal (line); amplitude and phase for $F = 1$ (a,c) and 0.3 (b,d).

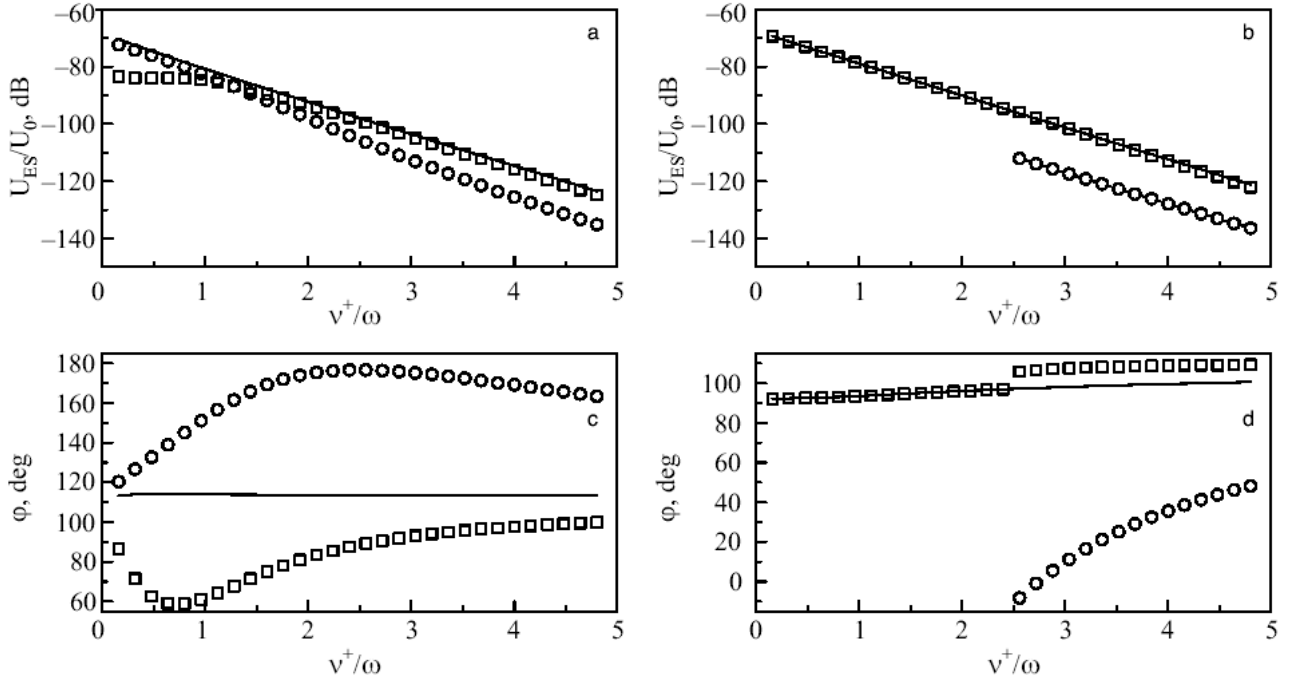


FIG. 8: Same as Fig. 7 for intense interband exchange ($v_1/v_0 = 0.6$), amplitude and phase for $F = 1$ (a,c) and 0.01 (b,d).

the phase changes of the resulting signal when a weak transverse magnetic field is applied was discussed in [16]. From the standpoint of the concept of the present work the result of [16] signifies that for a strong FLI the phase of the total signal should be expected to decrease and vice versa. However,

the separation in [16] was already made at the stage where the corresponding equations were solved, and to confirm this result it is desirable to perform the calculations taking account of all factors participating in the formation of the total signal.

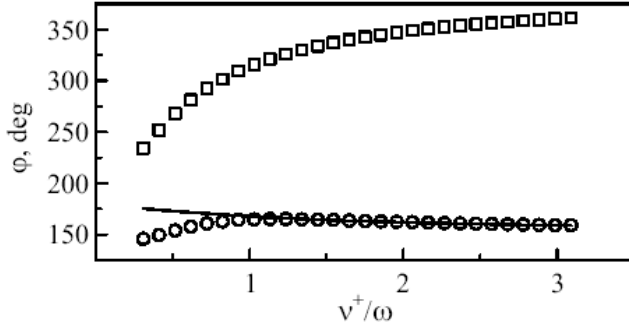


FIG. 9: Computed phases of the conversion coefficients; $v_1/v_0 = 0.03$, $F = 0.6$, $k_F x_0 = 1.2$: wave component (\circ), quasiwave component (\square), total signal (line).

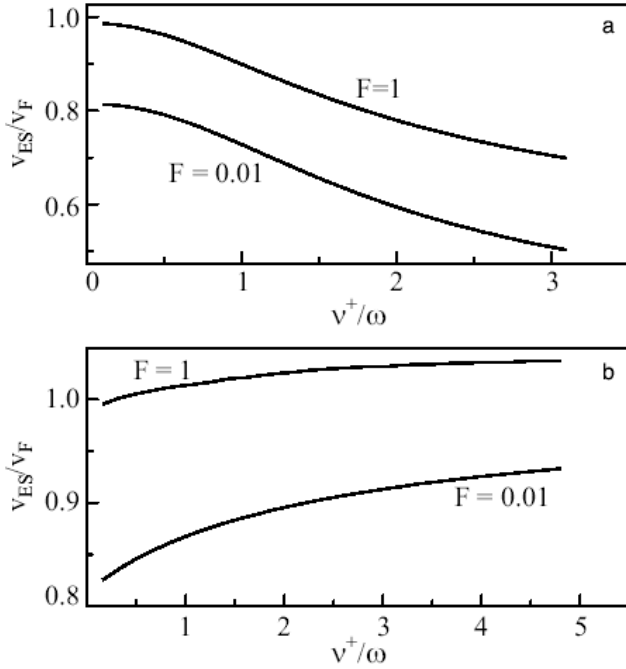


FIG. 10: Effect of the FLI on the velocity of electron sound: $k_F x_0 = 1.2$, $v_1/v_0 = 0.03$ (a) and $v_1/v_0 = 0.6$ (b).

IV. BEHAVIOR OF ELECTRON SOUND AT A SUPERCONDUCTING TRANSITION

In this very brief section we present the results of measurements of the characteristics of the electron sound propagation in a superconductor (Fig. 11). A completely unique conclusion follows from them – the observed amplitude and phase changes are independent of the thickness of the sample to within the accuracy of the measurements, i.e., the changes concern only the behavior of the transformation coefficient (or its square). In previous work [17] the decrease of the phase at T_c was mistaken for a change of the electron sound velocity, so that the conclusions based on this concept must be revised. Of course, the experimentally observed linear in the energy

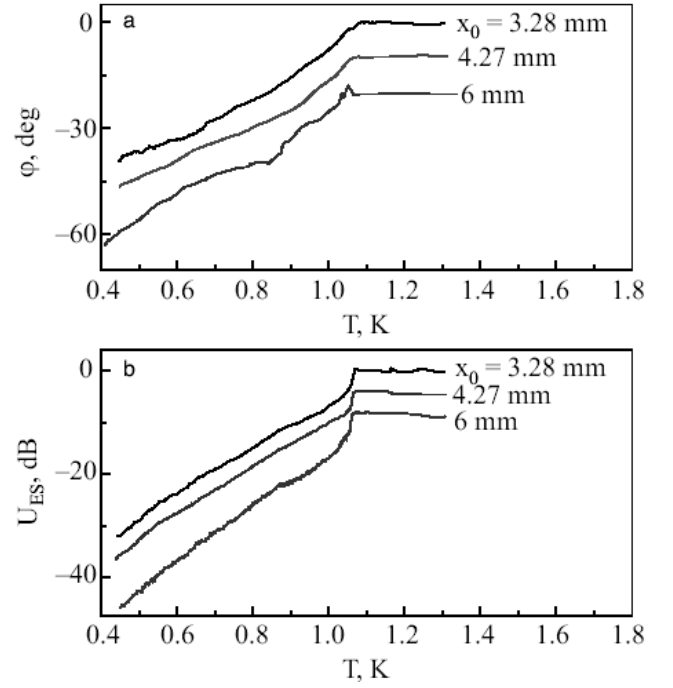


FIG. 11: Effect of a superconducting transition on the amplitude-phase characteristics of electron sound; the signal phases are shifted by 10 deg with respect to one another (a), amplitude (4 dB shift) (b)

gap phase change will remain, but the relation of the slope of this dependence with the FLI parameter must be determined more accurately. The evolution of the logarithm of the modulus of the transformation coefficient appears to be somewhat unusual for the kinetics of superconductors. The small jump is immediately followed by a wide linear section – as if its formation is determined by the so-called number of superconducting electrons [13].

Likewise, the results for the geometries $\mathbf{q} \parallel [010]$ and $\mathbf{q} \parallel [100]$ are practically identical in the superconducting phase (in contrast to the behavior in the normal state). This means that the anomalous interband exchange rate characteristic for the [010] axis plays no role in this case, just like the two-band structure may not play a role either. To some extent this makes it possible to validate the approach of Ref. 18, which is based on an analysis of the single-band model neglecting the FLI and relating the behavioral features of the electron sound below T_c with the evolution of the branch point contribution. However, even in this very simple case it is possible to come close to a solution of the problem only in the limit $|k_0| x_0 \gg 1$, which is far from the situation actually attainable in experiments. For this reason, on the whole, it can be stated that the processes determining the behavior of electron sound in a superconductor are not clearly understood at the present time.

V. CONCLUSION

We shall now formulate the essential results obtained in this work.

1. The amplitude-phase relations characterizing the propagation of electron sound in Ga samples of different length were studied. The modulus of the conversion coefficient and the temperature changes of the velocity of the wave and the phase of the transformation coefficient were determined.

2. A model problem of the excitation of electron sound in a finite-size sample with diffuse electron scattering at the interface boundaries was solved. It was shown that the character of the scattering has virtually no effect on the amplitude-phase characteristics of the propagating waves.

3. It was shown that the electronic pressure at the boundary of separation makes the main contribution to the recorded signal. As a result the amplitude of the displacements on the receiving interface is $v_F/2s$ times greater than that in the electron sound wave. This result is not limited to the phenomena discussed in the present work; it is valid for any case of the interaction of a wave, coupled with elastic deformations and moving with supersonic velocity, with an interface.

4. It was found that the changes occurring in the amplitude and phase of an electron sound wave in the superconducting phase are determined, first and foremost, by the evolution of the transformation coefficient and do not depend on the length of the sample.

We thank L. A. Pastur for helpful discussions and A. I. Petrishin for assisting in the measurements.

-
- [1] E. A. Kaner and V. G. Skobov, *Zh. Eksp. Teor. Fiz.* **43**, 610 (1963).
 - [2] L. P. Gorkov and I. E. Dzyaloshinskii, *Zh. Eksp. Teor. Fiz.* **44**, 610 (1963) [*Sov. Phys. JETP* **17**, 414 (1963)].
 - [3] A. I. Kopeliovich and M. S. Churyukin, *Fiz. Nizk. Temp.* **19**, 176 (1993) [*Low Temp. Phys.* **19**, 125 (1993)].
 - [4] E. V. Bezuglyi, N. G. Burma, E. Yu. Deineka, and V. D. Fil, *Fiz. Nizk. Temp.* **19**, 667 (1993) [*Low Temp. Phys.* **19**, 477 (1993)].
 - [5] G. I. Ivanovski and M. I. Kaganov, *Zh. Eksp. Teor. Fiz.* **83**, 2320 (1982) [*Sov. Phys. JETP* **56**, 1345 (1982)].
 - [6] E. V. Bezuglyi, *Fiz. Nizk. Temp.* **9**, 543 (1983) [*Low Temp. Phys.* **9**, 277 (1983)].
 - [7] N. G. Burma, A. I. Petrishin, N. A. Ryabukha, and V. D. Fil, *Fiz. Nizk. Temp.* **32**, 1507 (2006) [*Low Temp. Phys.* **32**, 1147 (2006)].
 - [8] E. V. Bezuglyi, N. G. Burma, E. Yu. Deineka, and V. D. Fil, *Fiz. Nizk. Temp.* **19**, 300 (1993) [*Low Temp. Phys.* **19**, 211 (1993)].
 - [9] E. A. Kaner, V. L. Falko, and L. P. Salnikova, *Fiz. Nizk. Temp.* **12**, 831 (1986) [*Low Temp. Phys.* **12**, 471 (1986)].
 - [10] A. S. Kondratev and A. E. Kuchma, *Lectures on the Theory of Quantum Liquids*, Leningrad University Press, Leningrad (1989).
 - [11] V. M. Kontorovich, in *Conduction Electrons*, Nauka, Moscow (1985).
 - [12] N. A. Zimbovskaya and V. I. Okulov, Preprint No. 275077, VINITI (1977).
 - [13] A. A. Abrikosov, *Principles of the Theory of Metals*, Nauka, Moscow (1987).
 - [14] B. Noble, *Methods Based on the WienerHopf Technique*, Pergamon Press, NY (1959).
 - [15] V. V. Furduyev, *Electroacoustics*, OGIZ, Moscow (1948).
 - [16] E. V. Bezuglyi, A. V. Boichuk, N. G. Burma, and V. D. Fil, *Fiz. Nizk. Temp.* **21**, 633 (1995) [*Low Temp. Phys.* **21**, 493 (1995)].
 - [17] E. V. Bezuglyi, N. G. Burma, E. Yu. Deineka, and V. D. Fil, *Sverkh. Fiz., Khim., Tekh.* **4**, 661 (1991).
 - [18] E. V. Bezuglyi and A. V. Boichuk, *Fiz. Nizk. Temp.* **23**, 676 (1997) [*Low Temp. Phys.* **23**, 507 (1997)].

* Electronic address: fil@ilt.kharkov.ua